ENHANCING 3D MOBILE ROBOT NAVIGATION: DQMD-DNN-BASED MOTION PLANNING WITH 3D MAPPING

Revannath B Kakade
Lecturer in Government Polytechnic Aurangbad
revankakade09@gmail.com India

Dr. KS Nagla, PhD
Associate Professor
Department of Instrumentation & Control Engineering,
Dr BR Ambedkar National Institute of Technology, Jalandhar
Punjab-India 144011

Abstract: For environment monitoring without human intervention, autonomous 3D mobile robot mapping is widely utilized. But, poor performance has been shown by the prevailing techniques in the complex environment. Thus, to deal with this limitation, a novel framework named 3-Dimensional Mobile Robot Mapping and Motion Planning using Deep Q-Learning-based Markov Decision Model Deep Neural Network(DQMD-DNN) (3DMRM-MP) is proposed. Here, the primary sensors are utilized for robot navigation. Afterward, the point clouds are pre-processed and the similar pixels are grouped together; then, features are extracted. The Gazelle Optimization Algorithm(GOA) is utilized for enhancing the feature extraction phase. Next, the current posture of the robot is estimated by the Transformation matrix applied Single value decomposition Linear N-Point Camera Pose Estimation (TMSVDLCPE); also, grounded on the estimated pose, the desired view is captured. The captured images are then converted into 3D formats. The robot's 3D images, speed, and current position are inputted to the DQMD-DNN, which efficiently plans the next optimal move of the robot. The experimental outcomes exhibited that the proposed technique withstands higher decision accuracy when contrasted with the prevailing frameworks.

Keywords: *Light Detection and Ranging (LIDAR); Inertial Measurement Unit (IMU); Brownian motion (BM); Bayes Distribution-Gazelle Optimization algorithm (BD-GOA); Deep Q-Learning-based Markov Decision Model Deep Neural Network (DQMD-DNN).*

1. INTRODUCTION

Strong mobility, precise positioning, simple structures, and simple control are several advantages of an omnidirectional mobile robot (C. Wang et al., 2020). The basic problem of mobile robots is their navigation capability. By identifying starting point and an end target point, the optimal path is selected (Perminov et al., 2021). In the past few decades, autonomous robots, specifically wheeled mobile vehicles, have made rapid progress (G. Xue et al., 2022). In GPS-denied environments, a Simultaneous Localization And Mapping (SLAM) system is needed primarily for the completion of such tasks (W. Wang et al., 2022). Afterward, for deciding which location would be the next best goal, an exploration module that employs the obtained map and the localized robot is required (Zhu et al., 2020).

The mapping quality has not been considered by the prevailing strategies (Yang et al., 2023). By identifying the paths with the maximum clearance from obstacles, fixed paths are generated by the Generalized Voronoi Diagram (GVD) path planner for any fixed environment, unlike the previous path-planning techniques (Jud et al., 2021). But, little work studied on how to establish a standard system for integrating and analyzing a variety of constraints that influenced robot navigation (Qi et al., 2022). However, this domain has 2 major limitations, namely (1) designing effective image features for expressing image information and (2) possible failure in cases of illumination change, camera parameter change, object movement, and single environments that lack texture (Xu et al., 2021) (W. Xue et al., 2020).

1.1. ***Problem Statement***

The work is motivated by,

- ❖ While using LIDAR for mapping, the result was accurate but of poor quality; this focused on enhanced mapping.
- ❖ In unknown environments, manual control is required for crawling, which may result in inaccurate decisions.

2694

Eur. Chem. Bull. 2023,12(10), 2694-2706

❖ For most of the algorithms, the exploration time was longer than usual.

1.2. Objectives

- The proposed technique enhanced the LIDAR-based Mapping Quality by utilizing an efficient preprocessing step.
- The proposed system developed robust decision-making systems that can effectively handle crawling in unfamiliar or challenging terrains, ensuring accurate and reliable navigation even without human intervention.
- The proposed method developed efficient exploration strategies in path planning techniques. The aim is to optimize the exploration time without compromising the accuracy and coverage of the mapping process.

This paper is organized as: Section 2 surveys the related work; Section 3 elucidates the proposed system; Section 4 illustrates the outcomes and discussion. Lastly, the paper is winded up in section 5.

2. LITERATURE SURVEY

(Gobhinath et al., 2021) propounded SLAM and middleware concepts like open source (ROS). For the cost at which the presented mechanism was constructed, this distance was very higher. But, arrangement files were well-defined with setup limitations as well as startups so that the equipment was to be wielded.

(Shin & Na, 2020) proffered an approach for displaying the elevation and temperature of a surveillance area in the form of a map by utilizing the Convolution Neural Network (CNN) algorithm. Outcomes displayed a better detection rate. Nevertheless, the reconstruction error for the primary anomaly was higher.

(Diane et al., 2019) established multi-aspect mapping technology at the level of their semantic representation. The developed mapping subsystem's inputs were a series of Red Green Blue-Depth (RGB-D) streams. However, while using large sets, the time extends and creates unwanted classes.

(Noh et al., 2020) introduced a system that could autonomously navigate an unstructured indoor environment, which avoided collision with static or else dynamic objects. Although it performed well in collision avoidance, still infer about object intentions was lower.

(Huang et al., 2019) developed a technique of concurrent construction of 2D as well as 3D maps grounded on the mobile robot. For achieving the robot's pose, the particle filter approach was wielded, which had superior performance. Yet, the map resolution was very low.

(Tang et al., 2020) presented a 3D exploration system centered on the wavefront framework. The experimental results demonstrated a higher efficacy. But, under the people's direct control of the environment, mapping could not be completed by mobile robots.

(Eldemiry et al., 2022) propounded an exploration technique for concurrently optimizing exploration time by utilizing a lower-cost RGB-D camera. Owing to low computational cost and low exploration time, feature-centric RGB-D SLAM was wielded. Nevertheless, the online mapping quality was lower.

3. PROPOSED METHODOLOGY FOR 3D MOBILE ROBOT MAPPING AND PATH PLANNING

The proposed model efficiently identifies the obstacles in the robot's path and makes optimal decisions for navigation, such as choosing a new path or adjusting the robot's speed and direction. Figure 1 elucidates the proposed system architecture.
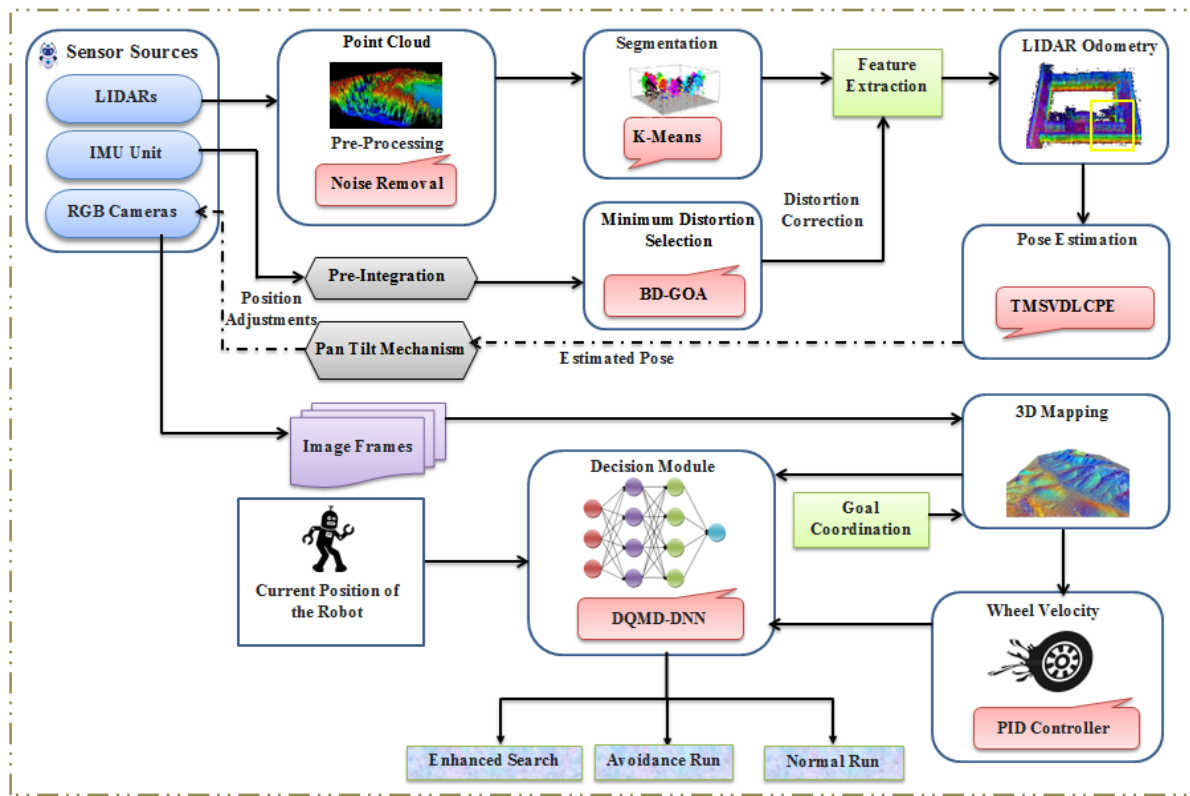
Figure 1: Architecture of the proposed framework

3.1. Sensor sources

LIDAR: LIDARs are utilized for mapping, localization, and navigation. It creates a point map (point cloud) of its surroundings.

Inertial Measurement Unit (IMU): It measures linear acceleration, angular velocity, and the magnetic field around the robot respectively.

RGB cameras: The images captured by the RGB cameras aid the robot identify objects and features in its surroundings.

3.2. Preprocessing

The point clouds from the LIDARs are preprocessed for removing noise and enhance the resulting point cloud's quality using a Gaussian Filter (GF). The GF is defined by,

$$G(a,b,c) = \left(\frac{1}{2\pi SD^3}\right) * Exp\left(-\left(\frac{a^2 + b^2 + c^2}{2SD^3}\right)\right)$$

$$(1)$$

Where, a, b and c are the pixel coordinates and SD exemplifies the standard deviation. The preprocessed point cloud is P_c.

3.3. Segmentation

Grounded on the pixel similarity, the pixels from P_c are grouped together using the K-Means algorithm, which is scalable to large datasets. The grouping of pixels aids the robot to understand the environment structure in a better way. The initial cluster centroid (Cn_i) is selected randomly. The pixels (Px_i), which have a minimum distance with (Cn_i), are assigned to the clusters. The clustering distance $(Dist)$ is computed by,

2696

Eur. Chem. Bull. 2023,12(10), 2694-2706

$$Dist_i = \sqrt{\sum_{i=1}^{n}(Cn_i - Px_i)^2}, \qquad Dist_i, i = 1,2,3,......,n$$

(2)

Here, i implies iteration.

3.4. Distortion correction

When a robot moves through its environment, the motion can cause distortions in the point cloud, which make it difficult to accurately extract features. Thus, to deal with this, pre-integrated IMU outputs are wielded that correct the distortions and enhance the feature extraction accuracy. The pre-integrated IMU outputs represent the expected change in orientation and position of the robot over a while. Therefore, the minimum distortions (M_d) are selected by BD-GOA. The GOA can avoid local optima and get a globally optimal solution. The GOA uses BM in the exploitation phase. However, the unequal step length in BM might lead to false convergence. To overcome this, Bayes Distribution (BD) is employed for the step length of BM. The steps of BD-GOA are defined further,

Primarily, the gazelle population (represents the position of the robot over a time ($p_{i,j}$)) is initialized by,

$$p_{i,j} = r \times (Ub_j - Lb_j) + Lb_j$$

(3)

Where, r is a random number, Ub_j and Lb_j are upper and lower bound, correspondingly.

After that, the fitness Ft is computed grounded on the minimum distortion $Min(Ds)$, which is referred to as,

$$Ft = Min(Ds)$$

(4)

Exploitation: When the gazelles are stalked by predators while grazing, the gazelles move in BM, this process is defined by,

$$\vec{g}_{i+1} = \vec{g}_i + k \cdot \vec{R} * \vec{B}_R * (\vec{E}_i - \vec{B}_R * \vec{g}_i)$$

(5)

Where, $\vec{g}_{i+1}$ and $\vec{g}_i$ are the solution of the next iteration and current iteration, correspondingly, k symbolizes grazing speed, $\vec{E}_i$ implies elite, $\vec{R}$ is random numbers in [0, 1], and $\vec{B}_R$ is a BM value. In BM, the step length is determined by BD,

$$Pb(St|L) = Pb(L|St) * Pb(St)/Pb(L)$$

(6)

Where, $Pb(St)$ is the prior probability of step length, $Pb(L)$ is the total probability of overall step length.

Exploration: Once the predator is spotted, the gazelle runs, and the predator chases. The sudden change of direction u is,

$$\vec{g}_{i+1} = \vec{g}_i + K \cdot u \cdot \vec{R} * \vec{L}_R * (\vec{E}_i - \vec{L}_R * \vec{g}_i)$$

(7)

Where, K describes the top speed of gazelle and $\vec{L}_R$ signifies Lévy distributions. The behaviour of the predator chasing the gazelle is displayed as,

2697

$$\vec{g}_{i+1} = \vec{g}_i + K \cdot u \cdot cf * \vec{B}_R * \left(\vec{E}_i - \vec{L}_R * \vec{g}_i\right)$$

(8)

Where, $cf = \left(1 - \dfrac{itr}{Max_{itr}}\right)^{\left(2\frac{itr}{Max_{itr}}\right)}$ signifies the controlling parameter. Grounded on (M_d), the point cloud is corrected S_C.

Input: Position of the robot over a time $(p_{i,j})$

Output: Minimum distortion (M_d)

Begin

    Initialize the population $(p_{i,j})$

    Compute the fitness value (Ft)

    While $(i = 1 \, to \, i_{Max})$ **do**

        Update the gazelle's position using,
$$\vec{g}_{i+1} = \vec{g}_i + k \cdot \vec{R} * \vec{B}_R * \left(\vec{E}_i - \vec{B}_R * \vec{g}_i\right)$$

Re-compute the fitness value (Ft)

        If $(Ft == Satified)$

            End the iteration

        Else

            Update the gazelle's positionusing,
$$\vec{g}_{i+1} = \vec{g}_i + K \cdot u \cdot \vec{R} * \vec{L}_R * \left(\vec{E}_i - \vec{L}_R * \vec{g}_i\right)$$

        End if

        $\vec{g}_{i+1} == Ft$

    End while

    Return (M_d)

End

3.5. Feature extraction

From S_C, important features (F) like line (detect walls, objects edge, and other straight or curved features in the environment), gradient (detect changes in elevation or slope in the environment), along with spatial features (track objects in the environment) are extracted.

3.6. LIDAR Odometry

Afterward, the LIDAR odometry (OT) is constructed using F, which estimates the robot's position and orientation. This is important for robot navigation and localization.

To construct (OT), (F) are matched between consecutive LIDAR scans. Once the matched features are identified, their relative motion is estimated by,

$$OT = Arg \min \sum \left(D(F_X, F_Y)\right)^2$$

(9)

Where, D symbolizes Euclidean distance, F_X and F_Y are corresponding features in the point clouds.

3.7. Pose estimation

Grounded on the estimated motions (Es), the robot's current posture in an environment is determined using a TMSVDLCPE, which is computationally efficient. In LCPE, the Projection Matrix (PM) is wielded for

2698

estimating the camera pose. But, the PM can result in an incorrect estimation of the camera pose owing to degenerate cases. To overcome this issue, a Transformation Matrix (TM) is utilized. The steps are as follows:

Step 1: Normalize the odometry image points by,

$$c_1 = (c_1 - x_a)/fx_a \tag{10}$$

$$c_2 = (c_2 - x_b)/fx_b \tag{11}$$

Where, c_1 and c_2 are the normalized image coordinates, x_a and x_b are principal point coordinates, fx_a and fx_b are focal lengths.

Step 2: The measurement matrix $[M]$ is constructed from the normalized image points and 3D coordinates of the known points $[A], [B],$ and $[C]$.

$$[M] = \begin{bmatrix} [A] & [B] & [C] & 1 & 0 & 0 & 0 & -c_1[A] & -c_1[B] & -c_1[C] & -c_1 \\ 0 & 0 & 0 & 0 & [A] & [B] & [C] & -c_2[A] & -c_2[B] & -c_2[C] & -c_2 \end{bmatrix} \tag{12}$$

Step 3: The SVD of $[M]$ is computed, this yields left (L) and right (R) singular vectors (Sv). The SVD is,

$$M = L * Sv * R \tag{13}$$

Step 4: After that, TM is computed by,

$$Tm = \text{Im} * Rm \tag{14}$$

Step 5: Lastly, the camera pose is recovered by decomposing TM into the camera extrinsic matrix (Em) and the intrinsic matrix (Im) by,

$$[Em, \text{Im}] = rq(Tm(1:3)) \tag{15}$$

$$Tv = \text{Im}^{-1} * Tm(:4) \tag{16}$$

Where, rq is decomposition factor, Tv is translation vector, $Tm(1:3)$ selects all rows and the first three columns of Tm, and $Tm(:4)$ selects all rows and the fourth column of Tm. Therefore, the estimated pose is defined by Ep.

3.8. Pan tilt mechanism

Centered on Ep, the Pan Tilt mechanism controls the movement of the RGB to capture a desired view of the scene. The captured images are further processed to extract frontier and area information, which provides valuable insights about the environment.

3.9. 3D mapping

To navigate to a destination point, the captured images are converted into 3D maps along with the goal coordinates. 3D mapping allows robots to better understand their environment by creating a detailed map in three dimensions. With a 3D map of the environment, robots can more easily navigate to a destination point by calculating the most efficient path and avoiding obstacles. Moreover, the 3D map can provide valuable information about the terrain, such as the height of objects and the depth of water, which can be utilized for making more informed decisions about how to move through the environment.

3.10. Wheel velocity

2699

Eur. Chem. Bull. 2023,12(10), 2694-2706

From 3D mapping, the information, such as the method of movement, track deviation from the landmark, and desired landmark are inputted to the Proportional-Integral-Derivative,

(PID) controller, which adjusts the wheel velocity to attain desired motion. The PID controller is expressed as,

$$T = G_P * E(t) + G_I * \int E(t)dt + G_D * de(t)/dt$$

(17)

Where, the control parameter is notated as T, proportional, integral, and derivative gains are exemplified as G_P, G_I and G_D, correspondingly, the error rate at the time t is specified as $E(t)$, the error over time's integral is signified as $\int E(t)dt$, and the derivative of the error at t is elucidated as $de(t)/dt$.

3.11. Decision making

The robot's current position, current velocity, and 3D maps are inputted to the DQMD-DNN, which efficiently makes decisions about the optimal action to take, namely normal run, enhanced search, and avoidance run.

Reinforcement learning is used by the DQMD-DNN to train the DNN by iteratively adjusting the Q-values grounded on feedback from the environment. To maximize the reward function, this work uses MD. The MD explores the complex environment and adapts to change the environment over time, allowing it to continue learning and updating the optimal rewards. Hence, the algorithm makes better decisions about how to navigate the environment over time. Figure 2 displays the DQMD-DNN architecture.
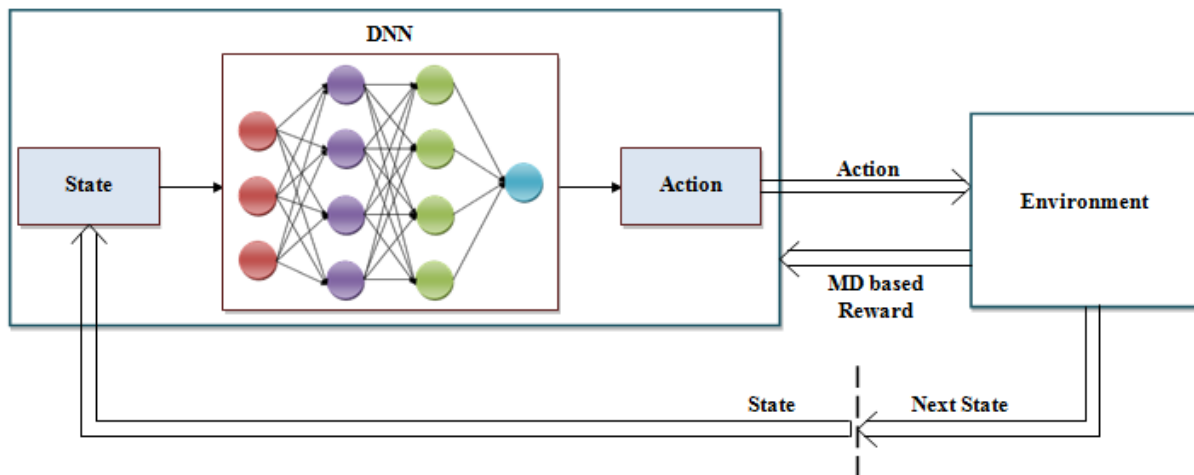

Figure 2: DQMD-DNN architecture

Afterward, the Q-values for each possible action are computed. The expected reward to take a specific action in the current state is represented by the Q-values.

$$Q(s,a) = Rw\pi(s,a) + \gamma * Max[Q(\bar{s}, \bar{a})]$$

(18)

Where, the Q-value of the current state (s)-action pair (a) is notated as $Q(s,a)$, γ defines discount factor, $Max[Q(\bar{s}, \bar{a})]$ is the maximum Q-value over all possible actions $\bar{a}$ in the next state $\bar{s}$, and $Rw\pi(s)$ is the reward obtained MD, this is given by,

$$Rw\pi(s) = ex\pi[Rw_{t+1} + \gamma Rw\pi\bar{s}]$$

(19)

Where, $ex\pi[Rw_{t+1} + \gamma Rw\pi\bar{s}]$ is the expected reward for the next state, and the reward received for taking action in the state (s) is represented as Rw_{t+1}.

Then, the best action is selected grounded on the Q-values by,

2700

$$B^* = Arg\max - B(Q(s,a)) \tag{20}$$

Where, B^* is the best action, $Arg\max - B$ symbolizes the action, which maximizes the Q-value.

The Q-value is updated for B^* using the Q-learning update rule,

$$Q(s,a) = Q(s,a) + \beta(Or + \gamma MaxQ(\overline{s},\overline{a}) - Q(s,a)) \tag{21}$$

Where, the learning rate is exemplified as β, the observed reward is implied as Or, the discount factor for future rewards is notated as γ.

Lastly, the loss function (Ls) is determined by,

$$L = (Q(s,a) - y)^2 \tag{22}$$

Where, y is the target Q-value; the parameters are adjusted through back-propagation to minimize (Ls).

## 4. RESULTS AND DISCUSSION

Here, the experiments conducted in the working platform of MATLAB are presented.
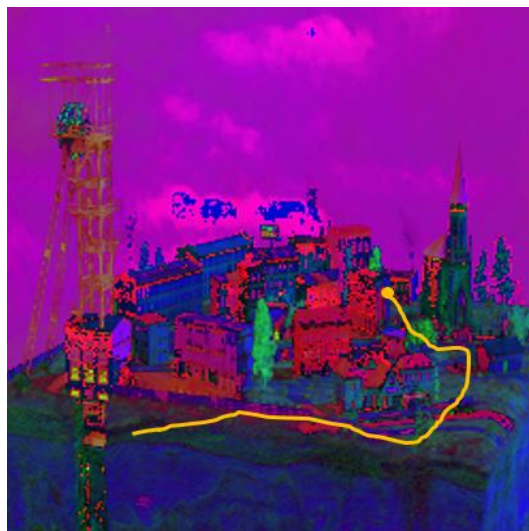
4.1. Dataset description

Toronto-3D, which is obtained by a Mobile Laser Scanning (MLS) system in Toronto, Canada for semantic segmentation, is a large-scale urban outdoor point cloud dataset. It approximately covers 1 km of road and comprises about 78.3 million points.

4.2 Performance Analysis

Here, the proposed 3DMRM-MP's performance is validated.
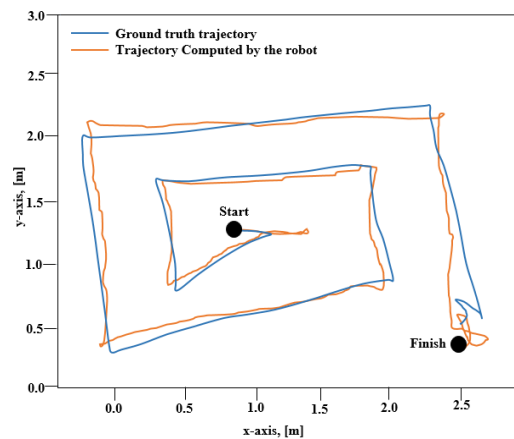
(a)

(b)

Figure 3 (a): Trajectory computation **(b)** Autonomous exploration of robot

The trajectory computed by the robot and the ground truth trajectory is compared in Figure3 (a), whereas the robot's autonomous exploration ability is displayed in Figure 3 (b). From the analysis, it is clear that the proposed system efficiently aids the robot in avoiding obstacles and passing safely in the exploration.

Table 1: Performance of the proposed 3DMRM-MP in terms of Frontier detection, Obstacle detection, and decision accuracy

Techniques	Performance metrics		
	Frontier detection	Obstacle detection	Decision accuracy
Proposed 3DMRM-MP	97.26	97.96	98.32

The proposed technique's performance is demonstrated in Table 1. The proposed 3DMRM-MP efficiently handles the distortions caused by the LIDARs. Furthermore, the proposed. 3DMRM-MP uses TMSVDLCPE for pose estimation and adjusts the RGB cameras as per the estimated results. Owing to this, the proposed 3DMRM-MP achieves 97.26% of frontier detection, 97.96% of Obstacle detection, and 98.32% of decision accuracy.

Table 2: Performance of the proposed 3DMRM-MP in terms of error rates

Techniques	Performance metrics		
	RMSE	Localisation error	Loss value
Proposed DQMD-DNN	1.76	2.36	1.68
DNN	6.78	7.34	4.87
RNN	9.38	10.58	6.74
LSTM	13.06	15.69	9.38

The proposed DQMD-DNN's performance is demonstrated in Table 2. The proposed DQMD-DNN is efficiently learned by the Deep Q-Learning method. Further, better rewards are selected by employing the MD technique. Hence, the RMSE, Localisation error, and Loss value of the proposed DQMD-DNN are 1.76%, 2.36%, and 1.68%, correspondingly. Therefore, the proposed DQMD-DNN is capable to make decisions with a limited error rate.
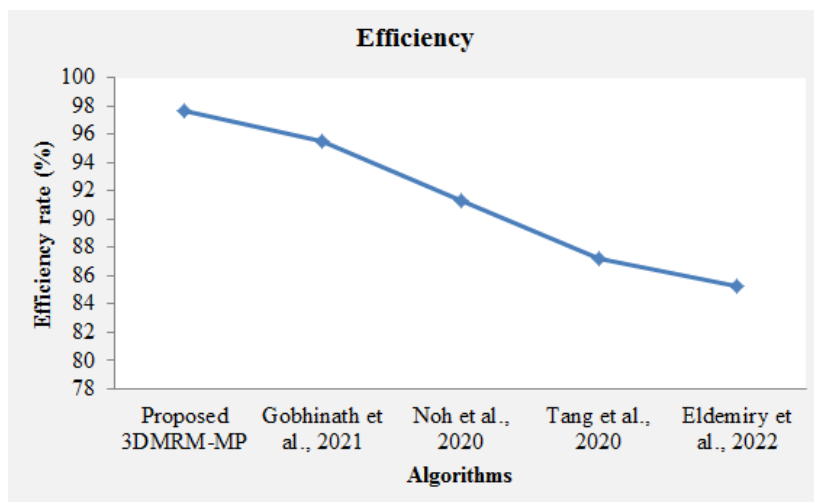
2702

Figure 4: Efficiency comparison

Figure 4 displays the efficiency of the proposed 3DMRM-MP and the conventional mechanisms. The proposed 3DMRM-MP efficiently corrects the distortion rates and maintains the RGB cameras to capture the desired location. As a result of this, the proposed technique's navigation efficiency is higher than the prevailing research
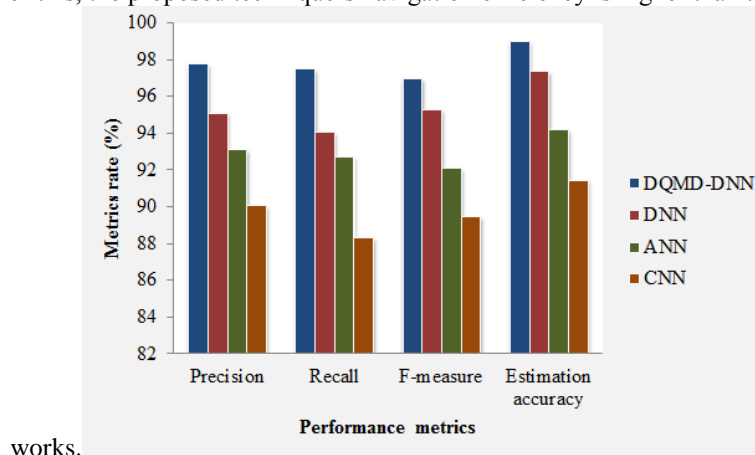

works.

Figure 5: Performance comparison

The proposed 3DMRM-MP and the conventional techniques' performance are exhibited in Figure 5. The proposed 3DMRM-MP efficiently selects the reward. Thus, the proposed 3DMRM-MP achieves precision, recall, F-measure, and Estimation accuracy of 97.8%, 97.5%, 97%, and 99%, correspondingly, whereas the existing techniques obtain lower performance rates. Hence, the proposed E-RS-GRU classifies the attacked and non-attacked data efficiently.
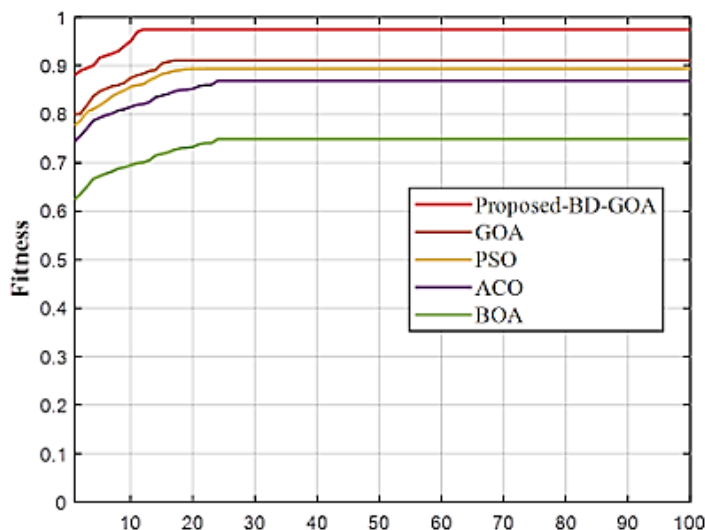
2703

Figure 6: Fitness vs. Iteration Comparison

Figure 6 compares the proposed BD-GOA's optimization ability with Particle Swarm Optimization (PSO), Butterfly Optimization Algorithm (BOA), GOA, along with Ant Colony Optimization (ACO). The proposed BD-GOA improves the exploration phase with the BD technique. Thus, the proposed BD-GOA renders the optimum outcome with a minimum number of iterations; however, to attain convergence, more iterations are required by the conventional mechanisms.

5. CONCLUSION

This paper proposed 3-dimensional mobile robot mapping and motion planning using DQMD-DNN. The system undergoes several operations like preprocessing, segmentation, Distortion correction, Feature extraction, Odometry creation, 3D mapping, and Decision making. Afterward, the experimental assessment is conducted, where the proposed system's performance, as well as comparative evaluation, is executed for validating the technique's efficacy. The presented framework could handle several uncertainties and renders more promising outcomes. For the assessment, the point cloud LIDAR (Toronto 3D) dataset is wielded, where the proposed system attains 98.32% of decision accuracy. This work mainly concentrated on 3D mobile robot mapping in an unknown environment with autonomous control; however, there are some undefined problems in real-time environments like sudden climatic changes, unpredictable holes in the ground, et cetera. In the future, the work could be focused to make decisions grounded on these sudden undefined changes also.

REFERENCES

Diane, S. A. K., Lesiv, E. A., Pesheva, I. A., & Neschetnaya, A. Y. (2019). Multi aspect environment mapping with a group of mobile robots. *Proceedings of the 2019 IEEE Conference of Russian Young Researchers in Electrical and Electronic Engineering*, *IEEE*, 478-482. https://doi.org/10.1109/EIConRus.2019.8656876

Eldemiry, A., Zou, Y., Li, Y., Wen, C. Y., & Chen, W. (2022). Autonomous exploration of unknown indoor environments for high-quality mapping using featurebased RGB-D SLAM. *Sensors*, *22*(14), 1-16. https://doi.org/10.3390/s22145117

Gobhinath, S., Anandapoorani, K., Anitha, K., Sri, D. D., & Divyadharshini, R. (2021). Simultaneous localization and mapping [SLAM] of robotic operating system for mobile robots. *7th International Conference on Advanced Computing and Communication Systems*, *1*, 577-580. https://doi.org/10.1109/ICACCS51430.2021.9441758

Huang, S., Li, C., Cai, Z., Zhu, G., Yao, L., & Fan, Z. (2019). Synchronized 2D SLAM and

2704

3D mapping based on three wheels omni-directional mobile robot. *Proceedings of the 9th IEEE International Conference on Cyber Technology in Automation, Control and Intelligent Systems*, 1177-1181. https://doi.org/10.1109/CYBER46603.2019.9066733

Jud, D., Hurkxkens, I., Girot, C., & Hutter, M. (2021). Robotic embankment. *Construction Robotics*, *5*(2), 101-113. https://doi.org/10.1007/s41693-021-00061-0

Noh, S., Park, J., & Park, J. (2020). Autonomous mobile robot navigation in indoor environments: Mapping, localization, and planning. *International Conference on Information and Communication Technology Convergence*, 908-913. https://doi.org/10.1109/ICTC49870.2020.9289333

Perminov, S., Mikhailovskiy, N., Sedunin, A., Okunevich, I., Kalinov, I., Kurenkov, M., & Tsetserukou, D. (2021). UltraBot: Autonomous mobile robot for indoor UV-C disinfection. *IEEE 17th International Conference on Automation Science and Engineering*, 2147-2152. https://doi.org/10.1109/CASE49439.2021.9551413

Qi, Y., Wang, R., He, B., Lu, F., & Xu, Y. (2022). Compact and efficient topological mapping for large-scale environment with pruned voronoi diagram. *Drones*, *6*(7), 1-12. https://doi.org/10.3390/drones6070183

Shin, H. C., & Na, K. (2020). Anomaly detection using elevation and thermal map for security robot. *International Conference on Information and Communication Technology Convergence*, 1760-1762. https://doi.org/10.1109/ICTC49870.2020.9289470

Tang, C., Liang, Y., Yu, S., Sun, R., & Zheng, J. (2020). Autonomous 3D exploration of indoor environment based on wavefront algorithm.*IEEE International Conference on Networking, Sensing and Control,* 1-6. https://doi.org/10.1109/icnsc48988.2020.9238092

Wang, C., Ma, H., Chen, W., Liu, L., & Meng, M. Q. H. (2020). Efficient autonomous exploration with incrementally built topological map in 3-D environments. *IEEE Transactions on Instrumentation and Measurement*, *69*(12), 9853-9865. https://doi.org/10.1109/TIM.2020.3001816

Wang, W., Jiang, L., Lin, S., Fang, H., & Meng, Q. (2022). Imitation learning based decision making for autonomous vehicle control at traffic roundabouts. *Multimedia Tools and Applications*, *81*(28), 39873-39889. https://doi.org/10.1007/s11042-022-12300-9

Xu, X., Wang, C., Wang, Y., & Xiong, R. (2021). *HiTMap:* A hierarchical topological map representation for navigation in unknown environments.*arXiv preprint*. http://arxiv.org/abs/2109.09293

Xue, G., Li, R., Liu, S., & Wei, J. (2022). Research on underground coal mine map construction method based on LeGO-LOAM improved algorithm. *Energies*, *15*(17), 1-17. https://doi.org/10.3390/en15176256

Xue, W., Ying, R., Gong, Z., Miao, R., Wen, F., & Liu, P. (2020). SLAM based topological mapping and navigation. *IEEE/ION Position, Location and Navigation Symposium*, 1336-1341. https://doi.org/10.1109/PLANS46316.2020.9110190

Yang, X., Lin, X., Yao, W., Ma, H., Zheng, J., & Ma, B. (2023). A robust LiDAR SLAM method for underground coal mine robot with degenerated scene compensation. *Remote Sensing*, *15*(1), 1-19. https://doi.org/10.3390/rs15010186

Zhu, J., Gehrung, J., Huang, R., Borgmann, B., Sun, Z., Hoegner, L., Hebel, M., Xu, Y., & Stilla, U. (2020). TUM-MLS-2016: An annotated mobile LiDAR dataset of the TUM city campus for semantic point cloud interpretation in urban areas. *Remote Sensing*, *12*(11), 1-18. https://doi.org/10.3390/rs12111875

2706

Eur. Chem. Bull. 2023,12(10), 2694-2706